

The Effective Mass Finder (EMAF) code

Patrizio Graziosi, School of Engineering, University of Warwick, UK

Permenent adress: CNR – ISMN, Bologna (Italy) Patrizio.Graziosi@cnr.it

Table of Contents

1. Overview	1
2. The effective mass concepts	2
3. The input data format	2
4. Code operation	3
5. Examples and applications	7

1. Overview

The Effective Mass Finder (EMAF) code aims to compute the meaningful effective mass parameters for a given, generic and arbitrary, three-dimensional (3D) bandstructure of semiconductors. In particular the EMAF code extracts the density of states (DOS) effective mass, m_{DOS} , and the conductivity effective mass, m_{cond} .¹⁻³ We introduce the meaning of the effective masses that the EMAF code computes, and the utilization of the code.

The code can be used by editing a text file or via a graphical user interface (GUI). The former is contained in a folder named “EMAF_v2 release” while the latter can be downloaded as an app anmed “EMAF_app”. The functionality is the same. In the folder “EMAF_v2” there is a script named “EMAF_run”; this is the only file that needs to be modified as explained in **section 4** and launched. When using the EMAF app, these instruction will be edited in the GUI.

In both cases, the code files are contained in a folder named “code”. “main_EMAF” is the main file that reads the entered instructions and drives all calculations. “shifting_bands_EMAF_funcnt” separates the conduction and the valence bands and prepare them for the next steps. “EMAF_DOS_funcnt” extracts the m_{DOS} . “nonSC_charge_calc_EMAF_3D_script” extracts the m_c . The band structures must be placed in the folder named “Bands”. The shape of these data and the information required are described in **section 3**. A third folder, “Extracion_from_bxs_f_v2”, contains a routine to extract the band structure form a .bxs_f file and compose them in the way required by the EMAF code, including the relative user guide.

The code is written in Matlab®, the user should have Matlab® and run the code as detailed below from the Matlab® desktop. The code is released open source under the GNU GPL v3.0 license. Every user should cite the code name and the web source.

2. The effective mass concepts

The m_{DOS} is the effective mass of an isotropic parabolic band that gives the same carrier density of the actual bandstructure as a whole.

The conductivity effective mass m_c is the effective mass of an isotropic parabolic band that gives the same injection velocity as a ballistic field effect transistor (FET) having a channel with the investigated bandstructure and operated in the subthreshold regime. Thus, m_{cond} grasps the essence of the bandstructure ballistic transport properties

3. The input data format

The EMAF code works on arbitrary and generic $E(\mathbf{k})$ expressed as a four dimensions (4D) matrix, where the first three dimensions are for the dimensions of the \mathbf{k} -space and the fourth dimension is for the band index. For instance, a band structure computed via DFT on a $61 \times 61 \times 41$ mesh for a material with 10 bands, will be understood as a $61 \times 61 \times 41 \times 10$ 4D matrix. On each (ix, iy, iz) point there 10 energy values that corresponds to the Hamiltonian eigenvalues and compose the ten bands, in this example. This matrix is labelled E_k . In the input bandstructure the Fermi level must be set to zero so that the code can automatically separate the conduction band and the valence band.

The code needs also the coordinates of the \mathbf{k} points to compute the band velocities and the volume integration element. They are considered as three 3D matrixes having the dimensions of the initial grid, $61 \times 61 \times 41$ in the former example. These matrixes are labelled `kx_matrix`, `ky_matrix` and `kz_matrix` and contains respectively the x , y and z coordinates in the \mathbf{k} space of the points that corresponds to the points of the E_k matrix. Thus, the kx coordinate of the point having numerical position (ix, iy, iz) is in `kx_matrix(ix, iy, iz)`, its ky coordinate in `ky_matrix(ix, iy, iz)` etc. and its ten energies of the former example, in `Ek(ix, iy, iz, 1:10)`. This is to express reciprocal unit cells, or Brillouin zones, or reciprocal unit cell, of arbitrary shape, onto a Cartesian axes system necessary to compute the transport quantities as tensors. **Figure 1** reports the reciprocal unit cell a Zincblende lattice. The discretization is done with a $4 \times 4 \times 4$ mesh for illustrative purpose. The \mathbf{a} , \mathbf{b} and \mathbf{c} axes of the reciprocal unit cell are shown. The right image is the view along the \mathbf{c} axis and shows the oblique shape and its relations with the orthogonal system. Each blue dot has three numerical indexes, ranging

from one to four in this case, that identify it along the first three dimension of the E_k matrix. The (x,y,z) Cartesian coordinates of each dot are in the kx_matrix , ky_matrix and kz_matrix respectively, where each dot is identified by the same three numerical indexes. The input file, labelled $Ek_material_name'$ (e.g. Ek_Mg3Sb2), shall contains these information. If the $k_matrixes$ are not provided, the k_arrays are needed and the code assumes orthogonal \mathbf{a} , \mathbf{b} , and \mathbf{c} axes to compose the $k_matrixes$.

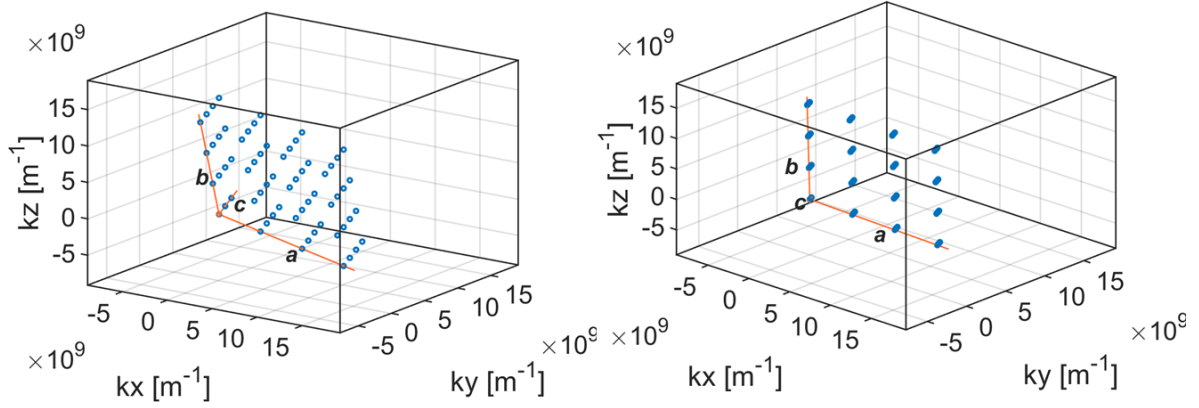


Figure 1: representation in Cartesian axes of a $4 \times 4 \times 4$ mesh that samples the reciprocal unit cell of a zincblende lattice. The oblique axes of the unit cell, \mathbf{a} , \mathbf{b} , and \mathbf{c} are reported.

4. The code operation

4.1 Extraction of the m_{DOS}

EMAF computes the m_{DOS} exploiting the facts that when the Fermi level is far from the band edge into the gap, the carrier density, per volume unit, can be expressed as

$$N = N_c e^{-\frac{E_c - E_F}{k_B T}} \quad (1)$$

In equation (1), E_c is the band edge, E_F the Fermi level, k_B the Boltzmann constant, T the temperature, $N_c = 2 \left(\frac{m_{DOS} k_B T}{2\pi\hbar^2} \right)^{3/2}$ the effective density of states in the conduction band.^{4,5} For a generic numerical bandstructure $E(\mathbf{k})$ where only the conduction bands is considered, we have:

$$N = \frac{2}{(2\pi)^3} \sum_{\mathbf{k}, n} f_{E_{\mathbf{k}, n}} dV_{\mathbf{k}} \quad (2)$$

where the sum runs over all the \mathbf{k} points in the reciprocal unit cell, or the Brillouin zone, and all the bands, $f_{E_{\mathbf{k}, n}}$ is the Fermi-Dirac distribution and $dV_{\mathbf{k}}$ is the volume element in the \mathbf{k} space that usually depends only on the mesh.⁵ Combining the equations (1) and (2), the effective density of states in the conduction band is obtained, then the m_{DOS} . The process is the same for the valence band, mutatis mutanda. The volume element is computed from the initial mesh as:

$$dV_k = (d\vec{k}_x \times d\vec{k}_y) \cdot d\vec{k}_z, \quad (3)$$

$$d\vec{k}_x = \left(\left(k_{x_{\text{matrix}(2,1,1)}}, k_{y_{\text{matrix}(2,1,1)}}, k_{z_{\text{matrix}(2,1,1)}} \right) - \left(k_{x_{\text{matrix}(1,1,1)}}, k_{y_{\text{matrix}(1,1,1)}}, k_{z_{\text{matrix}(1,1,1)}} \right) \right),$$

and similarly for $d\vec{k}_y$ and $d\vec{k}_z$, are the distance between two consecutive points in the reciprocal unit cell versus $x/y/z$. A regular mesh is required, so that the distance between one point and its nearest neighbors in the mesh, is the same everywhere.

4.2 Extraction of the m_c

The EMAF code computes the m_{cond} from the injection velocity $v_{\text{inj/sub}}$ of the carriers in the subthreshold regime of a FET,¹

$$m_{\text{cond}} = \frac{2k_B T}{\pi v_{\text{inj/sub}}^2} \quad (4).$$

A FET with the channel electronic bandstructure of the material under investigation is assumed, working separately for the conduction bands and the valence bands. A certain Source-Drain bias is imposed, that should be relatively large,² 1.5 eV have been used. Then the Fermi level is varied to mimic the gate bias application. The FET current I_{FET} , in units of current density, is computed from the difference between the Source and Drain currents for each band n :

$$I_{\text{FET}} = \sum_n (I_{S,n} - I_{D,n}) \quad (5)$$

where the Source and Drain currents $I_{S,n}$ and $I_{D,n}$ are calculated as

$$I_{S,n} = e \frac{1}{2} \frac{2}{(2\pi)^3} \sum_{k_n} f(E_{k_n} - E_{F,S}) v_{k_n} dV_k \quad (6a)$$

$$I_{D,n} = e \frac{1}{2} \frac{2}{(2\pi)^3} \sum_{k_n} f(E_{k_n} - E_{F,D}) v_{k_n} dV_k \quad (6b).$$

In the equations (6) e is the electron charge, the $1/2$ factor it introduced for total charge conservation, $E_{F,S}$ and $E_{F,D}$ are the Source and Drain Fermi levels respectively, whose difference corresponds to the Source-Drain applied bias, v_{k_n} is the carrier band velocity and f and dV_k are the Fermi-Dirac distribution and the volume element as in equation (2). Finally, the injection velocity is extracted as

$$v_{\text{inj}} = \frac{I_{\text{FET}}}{e \frac{1}{2} \frac{2}{(2\pi)^3} \sum_{k_n} f(E_{k_n} - E_{F,S}) dV_k} \quad (7).$$

The denominator in equation (7) is the injected charge at the Source contact. Then the $v_{\text{inj/sub}}$ is identified from the operational region of the FET and the conductivity effective mass is extracted from equation (4).

The above computation scheme is conducted along the three direction x , y , and z . Thus, three conductivity affective masses are extracted, $m_{\text{cond},x}$, $m_{\text{cond},y}$, and $m_{\text{cond},z}$ and a final average

conductivity effective mass is provided as $m_{\text{cond}} = \frac{3}{m_{\text{cond},x}^{-1} + m_{\text{cond},y}^{-1} + m_{\text{cond},z}^{-1}}$. EMAF applies this scheme separately for the conduction bands and the valence bands, *mutatis mutanda*.

The band velocities are computed from the gradient of the electron dispersions:

$$\mathbf{v} = \frac{1}{\hbar} \nabla_{\mathbf{k}} E = \frac{1}{\hbar} \left(\frac{\partial E}{\partial k_x}, \frac{\partial E}{\partial k_y}, \frac{\partial E}{\partial k_z} \right) \quad (8)$$

Thus, three 4D matrixes compose, V_x_{transp} , V_y_{transp} , V_z_{transp} , one for each of the three direction of the velocity vector field. The centred finite differences is the used method:

$$V_{x_{\text{transp}}(n_x, n_y, n_z, n_{\text{band}})} = \frac{E_{k(n_x+1, n_y, n_z, n_{\text{band}})} - E_{k(n_x-1, n_y, n_z, n_{\text{band}})}}{dk_{n_x}},$$

$dk_{n_x} = \text{abs} \left(\left(k_{x_{\text{matrix}}(n_x+1, n_y, n_z)}, k_{y_{\text{matrix}}(n_x+1, n_y, n_z)}, k_{z_{\text{matrix}}(n_x+1, n_y, n_z)} \right) - \left(k_{x_{\text{matrix}}(n_x-1, n_y, n_z)}, k_{y_{\text{matrix}}(n_x-1, n_y, n_z)}, k_{z_{\text{matrix}}(n_x-1, n_y, n_z)} \right) \right)$ is the distance along the x direction between the two points used to compute the finite differences.

The extracted values of the equivalent effective masses are displayed in the Matlab® desktop window.

4.3 Running the code, EMAF_run or the EMAF_app

Below we report the input instructions of the EMAF_run file.

```
% ----- input instructions -----
% -----
material_name = 'Mg3Sb2' ; % 'HfNiSn'; % 'Mg3Sb2' ; %
T = 300; % K

k_units_SI = 'yes'; % in 1/m
k_units_pi_a = 'no'; % for numerically built bands

Spin_Orbit_flag = 'off'; % if off, the two spins are equivalent, i.e. each
band contains two electrons

plot_velocities = 'yes'; % to plot automatically the injection velocities
% -----
% -----
```

The following figure displays the GUI app interface that asks for the same information.

Figure 2: GUI app to run the EMAF code without filling the text file. The instruction to be entered are the same.

`material_name` is the name of the material for which we want to compute the effective masses. Its band structure will be in a file named `Ek_'material_name'`.

`k_units_SI` and `k_units_pi_a` are to choose the units of the k axes between International Systems units, the former, or π/a , the latter. In the former case they are in units of m^{-1} , in the latter in π/a units and will be converted in m^{-1} . One of them shall be 'yes' and the other 'no'.

`Spin_Orbit_flag` allows setting if the bands are the same for majority and minority spins, 'off', or if they are spin resolved like in a ferromagnet, where the two spin orientations have different bands, 'on' case.

`plot_velocities` is 'yes' if we want the code to plot automatically the velocities. Figure 1 plots the carrier density versus Fermi level position. Figure 2 and Figure 3 plot the carrier injection velocities versus the carrier density and the Fermi level position, respectively. Figure 4 and Figure 5 display the current versus the carrier density, the former, or the Fermi level, the latter.

4.4 Subsidiaries quantities

In addition to the effective masses, the code computes other two quantities. The first is the weighted number of valleys per band, $\overline{n_v}$. This is the average number of valleys per band in the range of $5k_B T$ above the band edge; each valley is weighted for its occupancy quantified by the Fermi-Dirac distribution centred at the band edge. For each band, the total number of weighted valleys is computed and is then averaged across the bands with a minimum in the above energy range. The second quantity is a parameter computed as the product between the above weighted number of valley $\overline{n_v}$ and the average distance between them in the BZ, in units of $10^9 \text{m}^{-1} \overline{k_v}$. This parameter $p_v = \overline{n_v} \overline{k_v}$ aims at identifying at once band structures with many and far valleys, whose importance is explained in reference [3].

4.5 The saved quantities

The code displays the computed the effective masses, weighted average number of valleys and valleys parameter p_v . The code saves a file named `parameters_'material_name'` that contains the following quantities:

equivalent_DOS_mass_electrons, m_{DOS} for the CB
equivalent_DOS_mass_holes, m_{DOS} for the VB
equivalent_injection_mass_electrons, m_{cond} for the CB
equivalent_injection_mass_holes, m_{cond} for the VB
 k_dist_CB , $\overline{k_v}$ for the valleys in the CB
 k_dist_VB , $\overline{k_v}$ for the valleys in the VB
 me_inj_x , m_{cond} for the CB along the x direction
 me_inj_y , m_{cond} for the CB along the y direction
 me_inj_z , m_{cond} for the CB along the z direction
 mh_inj_x , m_{cond} for the VB along the x direction
 mh_inj_y , m_{cond} for the VB along the y direction
 mh_inj_z , m_{cond} for the VB along the z direction
 nv_CB , $\overline{n_v}$ for the valleys in the CB
 nv_VB , $\overline{n_v}$ for the valleys in the VB
 T , the used temperature
 vp_CB , p_v for the valleys in the CB
 vp_VB , p_v for the valleys in the VB.

5. Examples and applications

a. Parabolic bands

Parabolic bands with known analytical expression for the effective masses allow the code validation. We constructed numerical parabolic bands with isotropic effective mass of m_0 , and with anisotropic effective masses $m_x = m_0$, $m_y = 0.5m_0$, and $m_z = 0.1m_0$, where m_0 is the electron rest mass and compared the extracted masses with the known ones. We used a cubic mesh with spacing $dk = 0.02\pi/a$ where a is 0.5 nm. Table I shows a satisfactory agreement between the nominal values and the ones extracted by the EMAF code.

Band structure mass	Effective DOS mass		Effective conductivity mass	
	Nominal	Calculated	Nominal	Calculated
1 isotropic	1	0.9981	1	1.0078
1, 0.5, 0.1	0.3684	0.3677	0.2308	0.2463 (1.0078, 0.5079, 0.1085)

Table I: comparison between the nominal masses (in m_0 units) for the DOS and the conductivity, for isotropic and anisotropic bands. The values in parenthesis for the calculated conductivity masses in the anisotropic case are the three separated values extracted along the three space directions.

The concept and usefulness of the conductivity effective mass are depicted in **Figure 3**. Figure 2a shows the injection velocity versus carrier density for the cases of isotropic band, while Figures 2b and 2c report the transport distribution function (TDF) for elastic process with acoustic phonons via Acoustic Deformation Potential (ADP) and inelastic process via non-polar Optical Deformation Potential (ODP).⁷ We used the following scattering parameters: sound velocity $1.33 \cdot 10^3$ m/s, mass density $2 \cdot 10^3$ Kg/m³, ADP 10 eV, ODP $10 \cdot 10^{10}$ eV/m, $\hbar\omega_0$ 50 meV, temperature 300 K. An excellent agreement is achieved. Especially for the anisotropic case, Figure 2c, the TDF for the isotropic parabolic band having the conductivity effective mass extracted by the code reproduces very well the average TDF along the three directions. This demonstrates that the conductivity effective mass is the correct parameter to describe the transport properties of a bandstructure.

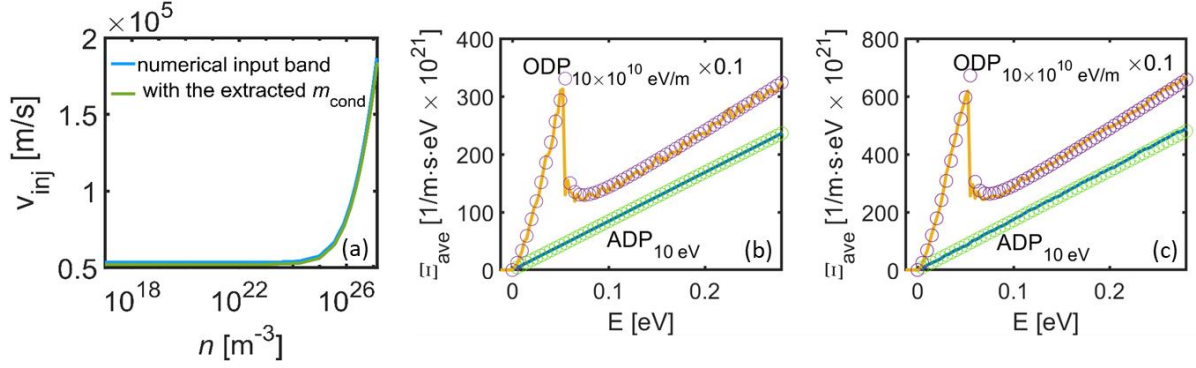


Figure 3: (a) injection velocity computed for the inputted numerical isotropic parabolic band (blue) and for an isotropic parabolic band with the effective mass extracted with the EMAF code. (b) and (c): average TDF Ξ_{ave} for isotropic (b) and anisotropic (c) bands, the average is along the three directions, the solid lines are the TDFs as numerically extracted with the code as in ref. [7], blue for the acoustic phonons, yellow for the optical phonons. The empty circles are the TDFs analytically computed for isotropic parabolic bands having the m_{cond} extracted with the code, green for the acoustic processes and purple for the inelastic ones.

b. Complex bandstructures

The case of the HfCoSb, especially of its valence band, constitutes a perfect example of complex bandstructure with many valleys and multiple minima. **Figure 4a** reports the numerical DOS for the HfCoSb, solid blue line, and the parabolic DOS that corresponds to the computed m_{DOS} values, dash-dot green line. The m_{DOS} concept catches the correct DOS trends at the band edge and represents an excellent and effective way to lump in a single parameter the richness of the bandstructure around the band onset.

The meaning of the m_c becomes clearer looking at the TDF computed for the actual numerical bandstructure and the TDF for an isotropic parabolic band with the effective mass equal to the extracted m_c , **Figure 4b**. The comparison makes sense for the isotropic scattering mechanisms only since in the parabolic approximation the distances between the \mathbf{k} points are obviously different. The blue solid line (numerical bandstructure) and the green dashed-dot line (parabolic band with m_{cond}) are for the ADP only mechanism. The m_c can clearly capture the transport properties of the complex bandstructure under elastic scattering at the band edge, when the DOS is parabolic-like. The inelastic ODP case, solid orange line (numerical bands) and purple dash-dot lines (parabolic band), presents a deviation related to the fact the final state DOS starts early to deviate from the parabolicity for phonon absorption. Thus, m_c can accurately describe the carrier velocity and transport properties, related to isotropic scattering with phonons, of complex bandstructures, close to the band edge. The m_{cond} concepts describes the transport properties of a complex electronic bandstructure in a single parameter.

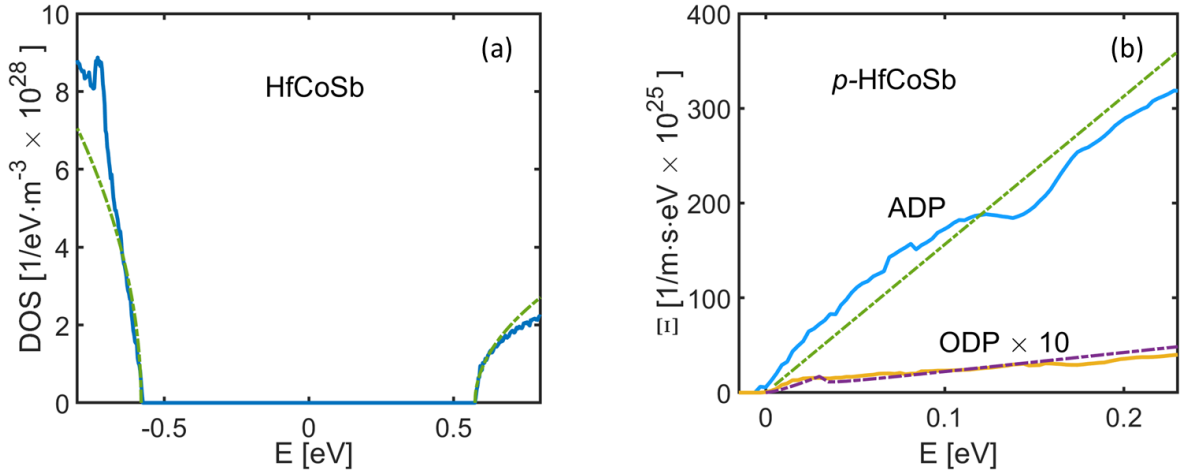


Figure 4: (a) DOS of HfCoSb, blue line, and DOS for parabolic bands with the isotropic m_{DOS} values, green dashed lines. (b) Transport distribution function versus energy of the HfCoSb valence band for the phonon processes ADP, Acoustic Deformation Potential, and ODP, Optical Deformation Potential, blue and yellow solid lines, respectively. The green and purple dashed lines represent the same quantity for a parabolic isotropic band having effective mass of m_{cond} .

Acknowledgement

This work has been funded by the Marie Skłodowska-Curie Actions under Grant Agreement No. 788465 (GENESIS – Generic semiclassical transport simulator for new generation thermoelectric materials).

References

- [1] Y. Liu, N. Neophytou, T. Low, G. Klimeck, and M. Lundstrom, *IEEE Trans. Electron Devices* 55, 866 (2008)
- [2] A. Rahman, J. Guo, S. Datta, M. Lundstrom, *IEEE Trans. Electron Devices* 50, 1853 (2003)
- [3] P. Graziosi, C. Kumarasinghe, N. Neophytou, *ACS Appl. Energy Mater.* 3, 5913 (2020)
- [4] R. F. Pierret, *Semiconductor Device Fundamentals*, Addison-Wesley, 1996, ISBN-13: 978-0201543933
- [5] M. Guzzi, “Principi di Fisica dei semiconduttori”. Hoepli, 2004, ISBN: 9788820333812
- [6] J. M. Ziman, “Principles of the Theory of Solids”, Cambridge University Press, 1965
- [7] P. Graziosi, C. Kumarasinghe, N. Neophytou, *J. Appl. Phys.* 126, 155701 (2019)